Available on CMS information server

CMS CR -2013/038

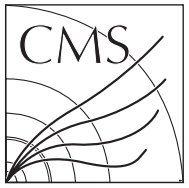

The Compact Muon Solenoid Experiment

Conference Report

Mailing address: CMS CERN, CH-1211 GENEVA 23, Switzerland

31 January 2013 (v2, 08 April 2013)

Search for H+- gt tau+nu with l+tau(- gt had) and ll final states in CMS

Pietro Vischia for the CMS Collaboration

Abstract

A search for a light charged Higgs boson is presented, conducted using $t\bar{t}$ events with $t \to bH^{\pm}$ and subsequent $H^{\pm} \to \tau^{\pm}\nu_{\tau}$ decay modes. The analysed data corresponded to an integrated luminosity of $\sim 2\ fb^{-1}$ recorded in proton-proton collisions at $\sqrt{s} = 7\ TeV$ by the CMS experiment at the LHC. The final states presented require the presence of a τ lepton from $H^{\pm}$ decays, an isolated lepton (e or μ) from $W^{\pm}$ decay and jets from the top quark decays. No excess of events was observed with respect to the expected SM background. Model-independent upper limits on the $t \to bH^{\pm}$ branching fraction were established in the range $2--4$ for charged Higgs boson masses between 80 and $160\ GeV$, under the assumption $\mathrm{B}(H^{\pm} \to \tau^{\pm}\nu_{\tau} = 1$. The limits were transformed in model-dependend upper limits on $tan(\beta)$ as a function of the charged Higgs mass, assuming the MSSM maximal mixing scenario.

Presented at *cHarged 2012 Fourth International Workshop on Prospects for Charged Higgs Discovery at Colliders*

PROCEEDINGS OF SCIENCE

Search for $H^{\pm} \to \tau^{\pm}\nu$ with $\ell + \tau(\to had)$ and $\ell\ell$ final states in CMS

Pietro VISCHIA[*†]
LIP-Lisboa
E-mail: pietro.vischia@gmail.com

A search for a light charged Higgs boson is presented, conducted using $t\bar{t}$ events with $t \to bH^{\pm}$ and subsequent $H^{\pm} \to \tau^{\pm}\nu_{\tau}$ decay modes. The analysed data corresponded to an integrated luminosity of ~ 2 fb^{-1} recorded in proton-proton collisions at $\sqrt{s} = 7$ TeV by the CMS experiment at the LHC. The final states presented require the presence of a τ lepton from $H^{\pm}$ decays, an isolated lepton (e or μ) from $W^{\pm}$ decay and jets from the top quark decays. No excess of events was observed with respect to the expected SM background. Model-independent upper limits on the $t \to bH^{\pm}$ branching fraction were established in the range $2 - -4\%$ for charged Higgs boson masses between 80 and 160 GeV, under the assumption B$(H^{\pm} \to \tau^{\pm}\nu_{\tau} = 1)$. The limits were transformed in model-dependend upper limits on $tan(\beta)$ as a function of the charged Higgs mass, assuming the MSSM maximal mixing scenario.

Prospects for Charged Higgs Discovery at Colliders
October 8-11, 2012
Uppsala University Sweden

[*]Speaker.
[†]on behalf of the CMS collaboration.

1. Introduction

The minimal supersymmetric extension of the standard model (MSSM) requires the introduction of two Higgs doublets in order that the superpotential can contain appropriate terms for giving masses to both up and down type quarks [1–8]. This leads to the prediction of five elementary Higgs particles: two CP-even (h,H), one CP-odd (A), and two charged ($H^{\pm}$) states [9, 10]. The lower limit on the charged Higgs boson mass is 78.6 GeV, as determined by LEP experiments [11–14]. If the mass of the charged Higgs boson is smaller than the difference between the masses of the top and the bottom quarks, i.e. $m_{H^+} < m_t - m_b$, the top quark can decay via $t \to H^+ b$ (charge conjugate processes are always implied throughout this paper). For values of $\tan\beta > 5$, the charged Higgs boson preferentially decays to a τ lepton and a neutrino, $H^+ \to \tau^+\nu_\tau$, where $\tan\beta$ is defined as the ratio of the vacuum expectation values of the two Higgs boson doublets. In deriving the experimental limits we assume that the branching fraction $\mathscr{B}(H^+ \to \tau^+\nu_\tau)$ is equal to 1.

The presence of the $t \to H^+ b$, $H^+ \to \tau^+\nu_\tau$ decay modes alters the τ lepton yield in the decay products of $t\bar{t}$ pairs compared to the standard model (SM). The upper limit on the branching fraction, $\mathscr{B}(t \to H^+ b) < 0.2$, has been set by the CDF [15] and D0 [16] experiments at the Tevatron for m_{H^+} between 80 and 155 GeV, assuming $\mathscr{B}(H^+ \to \tau^+\nu_\tau) = 1$. More recently, ATLAS experiment at the LHC has set the upper limit on the $\mathscr{B}(t \to H^+ b)$ between 5% and 1% for charged Higgs boson masses in the range 90–160 GeV [17].

The dominant process of production of top quarks at the Large Hadron Collider (LHC) is $pp \to t\bar{t}$+X via gluon gluon fusion. The search for a charged Higgs boson is sensitive to the decays of the top quark pairs $t\bar{t} \to H^{\pm}W^{\mp}b\bar{b}$ and $t\bar{t} \to H^{\pm}H^{\mp}b\bar{b}$, where each charged Higgs boson decays into a τ lepton and a neutrino. Throughout this paper, these two decay modes are referred to as WH and HH, respectively.

Two different final states were analyzed in [18] and are presented, all requiring missing transverse energy and multiple jets. The τ lepton decaying into hadrons and a neutrino is labeled τ_{h}. The first final state involves the production of τ_{h} in association with an electron or a muon (labeled $e\tau_{\mathrm{h}}$ or $\mu\tau_{\mathrm{h}}$), and the third one is where an electron and a muon are produced (labeled $e\mu$). Figure 1 shows representative diagrams for the $e(\mu)\tau_{\mathrm{h}}$ (left plot) and $e\mu$ (right plot) final states. The data samples used were recorded by the Compact Muon Solenoid (CMS) experiment until the end of August 2011 with an average number of interactions per crossing (pileup) of 5–6. The analyses correspond to an integrated luminosity ranging from 1.99 to 2.27 fb^{-1} depending on the final state.

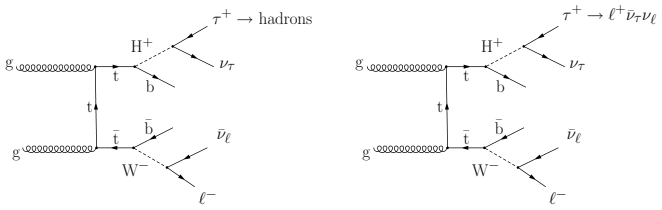

Figure 1: Representative diagrams for the τ_{h}+jets (left), $e(\mu)\tau_{\mathrm{h}}$ (middle), and $e\mu$ (right) final states.

2. CMS detector, reconstruction, and simulation

A detailed description can be found in Ref. [19]. The central feature of the CMS apparatus is a superconducting solenoid of $6m$ internal diameter providing a field of $3.8T$. Within the field volume are a silicon pixel and strip tracker, a crystal electromagnetic calorimeter (ECAL), and a brass/scintillator hadron calorimeter (HCAL). Muons are measured in gas-ionization detectors embedded in the steel return yoke of the magnet. Extensive forward calorimetry complements the coverage provided by the barrel and endcap detectors.

CMS uses a right-handed coordinate system, with the origin at the nominal interaction point, the x axis pointing to the centre of the LHC, the y axis pointing up (perpendicular to the LHC plane), and the z axis along the anticlockwise-beam direction. The polar angle θ is measured from the positive z axis and the azimuthal angle ϕ is measured in the x-y plane. The preudorapidity η is defined as $-\ln[\tan(\theta/2)]$.

The first level (L1) of the CMS trigger system, composed of custom hardware processors, uses information from the calorimeters and muon detectors to select the most interesting events in a fixed time interval of less than $4\mu s$. The High Level Trigger (HLT) processor farm further decreases the event rate from around $100kHz$ to around $300Hz$, before data storage.

Muons are reconstructed [20] by performing a simultaneous global track fit to hits in the silicon tracker and the muon system. Electrons are reconstructed [21] from clusters of energy deposits in the electromagnetic calorimeter that are matched to hits in the silicon tracker. Jets, τ_{h}, and missing transverse energy (E_T^{miss}) are reconstructed using particles measured with the particle-flow algorithm [22]. The particle-flow algorithm reconstructs particles in each event, using the information from the tracker, the ECAL and HCAL calorimeters, and the muon system. Jets are reconstructed with the anti-k_T jet algorithm [23] with a distance parameter of $R = 0.5$. The value of E_T^{miss} is defined as the magnitude of the vector sum of the transverse momenta of all reconstructed objects in the volume of the detector (leptons, photons, and hadrons).

The b-tagging algorithm used in this analysis exploits as the discriminating variable the significance of the impact parameter of the track with the second highest significance [24]. The significance is defined as the ratio of the measured value of the impact parameter to the measurement uncertainty. The hadron-plus-strips (HPS) τ identification algorithm [25] is used to reconstruct τ leptons decaying hadronically. The HPS algorithm considers candidates with one or three charged pions and up to two neutral pions. The τ_{h} candidate isolation is based on a cone of $\Delta R = \sqrt{\Delta\phi^2 + \Delta\eta^2} = 0.5$ around the reconstructed τ_{h}-momentum direction. It is required that no charged hadrons with $p_{\mathrm{T}} > p_{\mathrm{T}}^{\mathrm{cut}}$ and no photons with $E_T > E_T^{\mathrm{cut}}$ be present within the isolation cone, other than the τ_h constituents. The typical values of $p_{\mathrm{T}}^{\mathrm{cut}}$ and E_T^{cut} are $\simeq$1 GeV.

Backgrounds $t\bar{t}$, W+jets, Z+jets are generated with `MADGRAPH5` [26, 27] interfaced with `PYTHIA6.4.25` [28]. The diboson production processes WW, WZ, and ZZ are generated by `PYTHIA`. Single-top-quark production is generated with `POWHEG` [29]. The signal processes, $t\bar{t} \to HpmbH^{\mp}\bar{b}$ and $t\bar{t} \to W^{\pm}bH^{\mp}\bar{b}$, are generated by `PYTHIA`. The `TAUOLA` [30] package is used to simulate τ decays in all cases.

Generated events are processed through the full detector simulation based on `GEANT4` [31, 32], followed by a detailed trigger emulation and the CMS event reconstruction. Several minimum-bias events are superimposed upon the hard interactions to simulate pileup. The simulated events

are weighted according to the measured distribution of the number of interaction vertices. The PYTHIA parameters for the underlying event were set according to the "Z2" tune, an update of the "Z1" tune described in Ref. [33].

The number of produced $t\bar{t}$ events is estimated from the SM prediction of the $t\bar{t}$ production cross section, $165^{+4}_{-9}(\text{scale})^{+7}_{-7}(\text{PDF})pb$ [34 – 37]. The theoretical prediction agrees with the cross section measured at the LHC [38, 39].

3. Analysis of the $e\tau_h$ and $\mu\tau_h$ final states

In the $e\tau_h$ analysis, the events are selected by a trigger that requires the presence of an electron, at least two jets with $p_T > 30$ GeV and $p_T > 25$ GeV, respectively, and a certain amount of H_T^{miss}, where H_T^{miss} is defined at the trigger level as the magnitude of the vector sum of p_T of all jets in the event. As the peak instantaneous luminosity increased the requirements on the electron p_T changed from 17 to 27 GeV and on H_T^{miss} from 15 to 20 GeV. The amount of data analyzed for this channel corresponds to an integrated luminosity of $1.99 \pm 0.05\,\text{fb}^{-1}$

In the $\mu\tau_h$ analysis, the events are selected by a single-muon trigger with the threshold changing from 17 to 24 GeV during the data taking period. The amount of data analyzed for this channel corresponds to an integrated luminosity of $2.22 \pm 0.05\,\text{fb}^{-1}$.

The events are selected by requiring one isolated, high-p_T electron (muon) with $p_T > 35\,(30)$ GeV and $|\eta| < 2.5\,(2.1)$. The event should have one τ_h with $p_T > 20$ GeV within $|\eta| < 2.4$, at least two jets with $p_T > 35\,(30)$ GeV within $|\eta| < 2.4$, with at least one jet identified as originating from the hadronization of a b quark, and $E_T^{miss} > 45\,(40)$ GeV for the $e\tau_h$ ($\mu\tau_h$) final state. The τ_h and the electron (muon) are required to have opposite electric charges. The isolation of each charged lepton candidate (e or μ) is measured by summing the transverse momenta of the reconstructed particles within a cone of radius $\Delta R = 0.3$ around the lepton's direction. The contribution from the lepton itself is excluded. If the value of this sum divided by the lepton p_T, labeled I_{rel}, is less than 0.1 (0.2) for electrons (muons), the lepton is considered to be isolated. The lepton is required to be separated from any selected jet by a distance $\Delta R > 0.3$. Events with an additional electron (muon) with $I_{rel} < 0.2$ and $p_T > 15\,(10)$ GeV are rejected.

The backgrounds in the $e\tau_h$ and $\mu\tau_h$ final-state analyses arise from two sources, the first with misidentified τ_h, which is estimated from data, and the second with genuine τ_h, which is estimated from simulation. The misidentified τ_h background comes from events with one lepton (e or μ), E_T^{miss}, and three or more jets with at least one identified b quark jet (labelled "$\ell+ \geq 3$ jets" events), where one jet is misidentified as a τ_h. The dominant contribution to this background comes from W+jets, and from $t\bar{t} \to W^+bW^-\bar{b} \to \ell\nu b\, qq'\bar{b}$ ($\ell = e, \mu$) events. The misidentified τ_h background is estimated by applying the probability that a jet mimics a τ_h to every jet in "$\ell+ \geq 3$ jets" events. The probability that a jet is misidentified as a τ_h is measured from data as a function of jet p_T and η using W+jets and multijet events [25].

The backgrounds with genuine τ leptons are Drell–Yan $\tau\tau$, single-top-quark production, dibosons, and the SM $t\bar{t}$ events in which a τ is produced from a W decay. The $Z/\gamma^* \to ee$, $\mu\mu$ and $t\bar{t} \to W^+bW^-\bar{b} \to \ell^+\nu b\ell^-\bar{\nu}\bar{b}$ events may also contain electrons or muons misidentified as τ_h. The event yields for these backgrounds are estimated from simulation.

The data and the simulated event yield at various stages of event selection, described above, for the $e\tau_{\rm h}$ ($\mu\tau_{\rm h}$) analysis are shown in Fig. 2 left (right). The backgrounds are normalized to the SM prediction obtained from the simulation. A good agreement is found between data and the SM background. The expected event yield in the presence of $t \to H^+b$, $H^+ \to \tau^+\nu_\tau$ decays is shown as a dashed line for $m_{H^+} = 120$ GeV under the assumption that $\mathscr{B}(t \to H^+b) = 0.05$. The observed

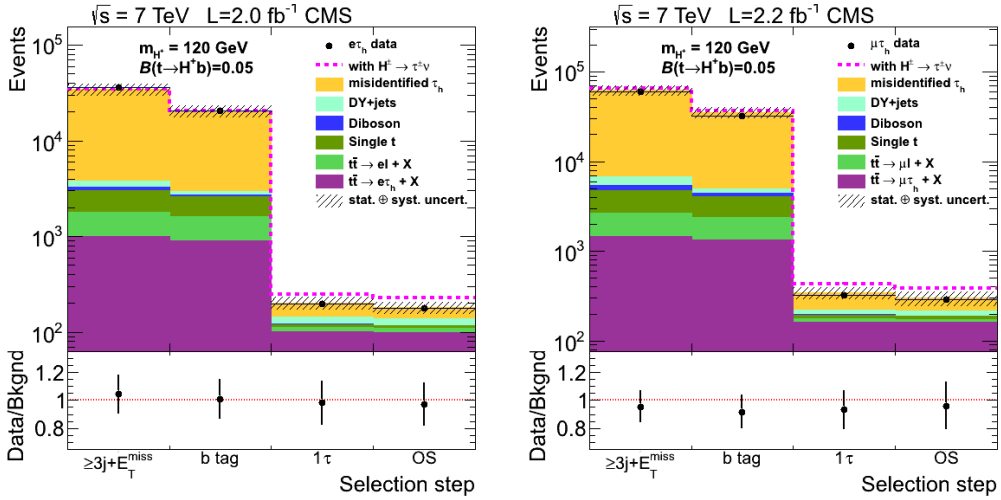

Figure 2: The event yields after each selection step for the $e\tau_{\rm h}$ (left) and $\mu\tau_{\rm h}$ (right) analyses. The backgrounds are estimated from simulation and normalized to the standard model prediction. The expected event yield in the presence of the $t \to H^+b$, $H^+ \to \tau^+\nu_\tau$ decays is shown as a dashed line for $m_{H^+} = 120$ GeV and under the assumption that $\mathscr{B}(t \to H^+b) = 0.05$. The bottom panel shows the ratios of data over background with the total uncertainties. OS indicates the requirement to have opposite electric charges for a $\tau_{\rm h}$ and a e or μ. Statistical and systematic uncertainties are added in quadrature.

number of events after the full event selection is shown in Table 1 along with the expected numbers of events from the various backgrounds, and from the Higgs boson signal processes WH and HH for $m_{H^\pm} = 120$ GeV. The misidentified τ background measured from the data is consistent with the expectation from simulation, $42 \pm 4(stat.) \pm 8(syst.)$ for the $e\tau_h$ analysis and $83 \pm 7(stat.) \pm 12(syst.)$ for the $\mu\tau_h$ analysis.

4. Analysis of the $e\mu$ final state

The $e\mu$ events are selected by a trigger requiring an electron with $p_{\rm T}^e > 8$ GeV and a muon with $p_{\rm T}^\mu > 17$ GeV; or an electron with $p_{\rm T}^e > 17$ GeV and a muon with $p_{\rm T}^\mu > 8$ GeV. The amount of data analyzed for this channel corresponds to an integrated luminosity of $2.27 \pm 0.05\,{\rm fb}^{-1}$.

In the $e\mu$ analysis, the events are selected by requiring at least one isolated electron and at least one isolated muon ($I_{\rm rel} < 0.15$) in a cone of radius $\Delta R = 0.3$ around the lepton with $p_{\rm T} > 20$ GeV within $|\eta| < 2.5\,(2.4)$ for electrons (muons). The event has to have at least two jets with $p_{\rm T} > 30$ GeV within $|\eta| < 2.4$. The leptons are required to be separated from any selected jet by a distance $\Delta R > 0.4$. The invariant mass of electron-muon pair, $m_{e\mu}$, is required to exceed 12 GeV. The electron and the muon are required to have opposite electric charges.

Table 1: Numbers of expected events in the $e\tau_h$ and $\mu\tau_h$ analyses for the backgrounds and the Higgs boson signal from WH and HH processes at $m_{H^+} = 120$ GeV, and the number of observed events after the final event selection. Unless stated differently, the expected background events are from simulation.

Source	$N_{ev}^{e\tau_h} \pm stat. \pm syst.$	$N_{ev}^{\mu\tau_h} \pm stat. \pm syst.$
HH+HW, $m_{H^+} = 120$ GeV, $\mathscr{B}(t \to H^+b) = 0.05$	$51 \pm 3 \pm 8$	$89 \pm 4 \pm 13$
misidentified τ (from data)	$54 \pm 6 \pm 8$	$89 \pm 9 \pm 11$
$t\bar{t} \to WbW\bar{b} \to \ell\nu b\ \tau\nu\bar{b}$	$100 \pm 3 \pm 14$	$162 \pm 4 \pm 23$
$t\bar{t} \to WbW\bar{b} \to \ell\nu b\ \ell\nu\bar{b}$	$9.0 \pm 0.9 \pm 1.8$	$13.0 \pm 1.2 \pm 2.5$
$Z/\gamma^* \to ee, \mu\mu$	$4.8 \pm 1.8 \pm 1.3$	$0.7 \pm 0.7 \pm 0.7$
$Z/\gamma^* \to \tau\tau$	$17.0 \pm 3.3 \pm 3.0$	$26.0 \pm 4.3 \pm 6.1$
single top quark	$7.9 \pm 0.4 \pm 1.1$	$13.5 \pm 0.5 \pm 1.9$
diboson	$1.3 \pm 0.1 \pm 0.2$	$2.0 \pm 0.2 \pm 0.3$
Total expected background	$194 \pm 8 \pm 20$	$306 \pm 11 \pm 32$
Data	176	288

The backgrounds considered in the $e\mu$ final-state analysis are the following: SM $t\bar{t}$, Drell–Yan $\ell\ell$ ($\ell = e, \mu, \tau$) production in association with jets (DY($\ell\ell$)), W+jets, single-top-quark production (dominated by tW) and diboson (WW, WZ, ZZ) production. Background yields are all estimated from simulation. After the signal selection requirements are applied, 95% of the remaining background is due to SM $t\bar{t}$ decays.

The data and simulated event yields at various stages of the event selection are shown in Fig. 3. The backgrounds are normalized to the standard model prediction obtained by simulation. A good agreement between the data and the standard model expectations is found. The expected event yield in the presence of $t \to H^+b$, $H^+ \to \tau^+\nu_\tau$ decays is shown as a dashed line for $m_{H^+} = 120$ GeV under the assumption that $\mathscr{B}(t \to H^+b) = 0.05$. It is smaller than the expectation from the SM alone ($\mathscr{B}(t \to H^+b) = 0$) because the selection efficiency is smaller for $H^+ \to \tau^+\nu_\tau \to \ell^+\nu_\ell\bar{\nu}_\tau\nu_\tau$ than for $W^+ \to \ell^+\nu_\ell$ decay owing to the softer lepton p_T spectrum.

The numbers of expected events for the backgrounds and the Higgs boson signal processes from WH and HH modes at $m_{H^\pm} = 120$ GeV, and the number of observed events after all selection requirements are summarized in Table 2.

5. Systematic uncertainties

In all the analyses the following effects are taken into account:

- the uncertainty on the jet energy scale (JES), jet energy resolution (JER), and E_T^{miss} scale. This uncertainty is estimated following the procedure outlined in Ref. [43]; an uncertainty of 3% on the τ_h energy scale is included;
- the theoretical uncertainties on the signal and background cross sections;
- the uncertainty on pileup modelling due to the reweighting of simulated events according to the measured distribution of the number of vertices;

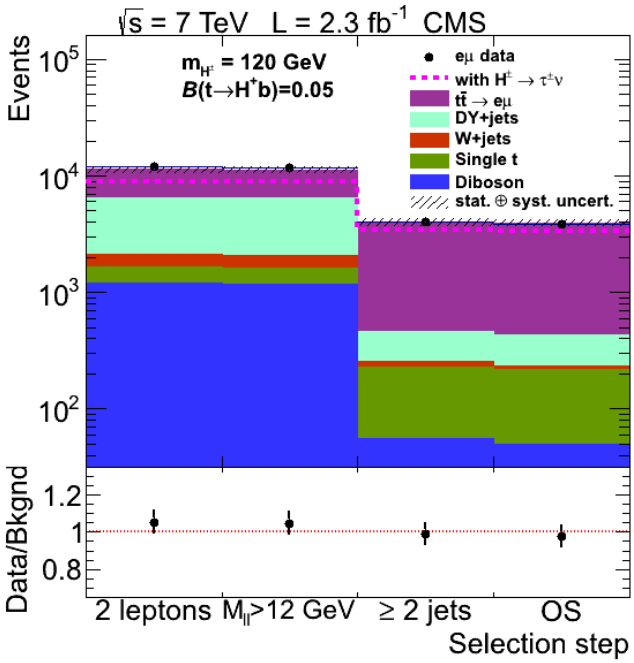

Figure 3: The event yield after each selection step for the $e\mu$ analysis. The backgrounds are from simulation and normalized to the standard model prediction. The expected event yield in the presence of the $t \to H^+b$, $H^+ \to \tau^+\nu_\tau$ decays is shown as a dashed line for $m_{H^+} = 120$ GeV under the assumption that $\mathscr{B}(t \to H^+b) = 0.05$. The bottom panel shows the ratios of data over background with the total uncertainties. The requirement for the e and μ to have opposite electric charges is labelled as OS. Statistical and systematic uncertainties are added in quadrature.

- the uncertainty due to the limited number of events available in the simulated samples (MC stat.);
- an estimated 2.2% uncertainty in the integrated luminosity.

In addition, for the analyses with τ_h in the final state (τ_h+jets, $e\tau_h$, $\mu\tau_h$), the following systematic uncertainties are taken into account:

- the uncertainty on the efficiency of τ identification, estimated to be 6% [25];
- the uncertainty on the rate of misidentification of a jet as a τ_h or of a lepton as a τ_h, each estimated to be 15% [25];
- the uncertainty on the efficiency of b tagging, 5.4% [24];
- the uncertainty on the rate of misidentification of a jet as a b quark, 10% [24].

In the $e\tau_h$ and $\mu\tau_h$ analyses the uncertainty in the estimation of the misidentified τ background has two sources: the limited number of events for the measurement of the τ misidentification rate and the difference in the τ misidentification rates for jets originating from a quark with respect to jets originating from a gluon.

Table 2: Number of expected events in the $e\mu$ analysis for the backgrounds, the Higgs boson signal from HH and WH processes at $m_{H^+} = 120$ GeV, and the number of observed events after all selection requirements. The expected background events are from simulation.

Source	$N_{\rm ev}^{e\mu} \pm$ stat. $\pm$ syst.
HH+WH, $m_{H^+} = 120$ GeV, $\mathscr{B}(t \to H^+ b) = 0.05$	$125 \pm 9 \pm 13$
$t\bar{t}$ dileptons	$3423 \pm 35 \pm 405$
other $t\bar{t}$	$23 \pm 3 \pm 3$
$Z/\gamma^* \to \ell\ell$	$192 \pm 12 \pm 19$
W+jets	$14 \pm 6 \pm 2$
single top quark	$166 \pm 3 \pm 18$
diboson	$48 \pm 2 \pm 5$
Total expected background	$3866 \pm 38 \pm 406$
Data	3875

Finally the uncertainty on the reconstruction, identification, and isolation efficiency of an electron or a muon is taken into account and estimated to be $\simeq$2–3%.

The full sets of systematic uncertainties are used as input to the exclusion limit calculation.

6. Evaluation of limits on $\mathscr{B}(t \to H^+ b)$

In the e$\tau_{\rm h}$ and $\mu\tau_{\rm h}$ analyses the total expected $t\bar{t}$ event yield from WW, WH, and HH processes is larger than the yield from the standard model $t\bar{t} \to WbW\bar{b}$ process . This is due to the fact that the branching fraction for the Higgs boson decay into $\tau\nu_\tau$ is larger than the corresponding branching fraction for W boson decay. For the $e\mu$ analysis the total $t\bar{t}$ event yield is smaller than that expected from the standard model.

Assuming that any excess or deficit of events in data, when compared with the expected background contribution, is due to the $t \to H^+ b$, $H^+ \to \tau^+\nu_\tau$ decays, the value of $x = \mathscr{B}(t \to H^+ b)$ for each individual analysis can be related to the difference ΔN between the observed number of events and the predicted background contribution

The CLs method [44, 45] is used to obtain an upper limit, at 95% confidence level (CL), on $x = \mathscr{B}(t \to H^+ b)$. The background and signal uncertainties described in Section 5 are modeled with a log-normal probability distribution function and their correlations are taken into account. The event counting, together with the nuisance parameters which model the background and signal uncertainties, is used to obtain the upper limits.

The upper limit on $\mathscr{B}(t \to H^+ b)$ as a function of m_{H^+} is shown in Fig. 4 for the $\mu\tau_{\rm h}$ and $e\tau_{\rm h}$ final states and in Fig. 5 for the and $e\mu$ final state. The combined upper limit has been obtained using the procedure described in [46]. Figure 6 (left) shows the upper limit obtained from the combination of all the presented final states together with the limit obtained in the $\tau_{\rm h}$ + jets final state examined in [18].

Table 3 gives the values of the median, $\pm 1\sigma$, and $\pm 2\sigma$ expected and the observed 95% CL upper limit for $\mathscr{B}(t \to H^+ b)$ as a function of m_{H^+} for the combination of the fully hadronic, $e\tau_{\rm h}$,

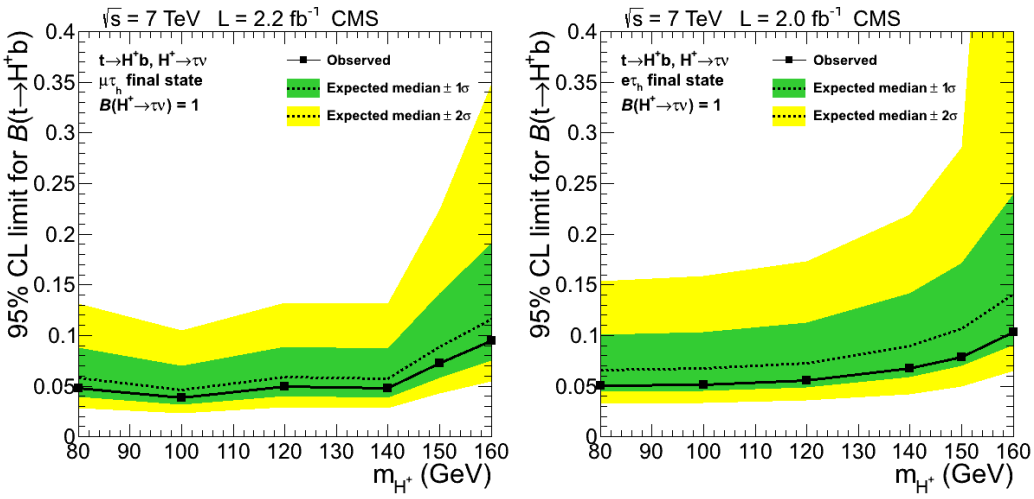

Figure 4: Upper limit on $\mathscr{B}(t \to H^+b)$ as a function of m_{H^+} for the $\mu\tau_{\rm h}$ (left) and the $e\tau_{\rm h}$ (right) final states. The $\pm1\sigma$ and $\pm2\sigma$ bands around the expected limit are also shown.

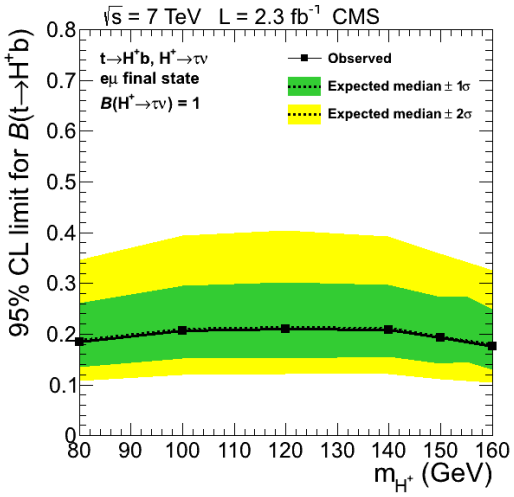

Figure 5: Upper limit on $\mathscr{B}(t \to H^+b)$ as a function of m_{H^+} $e\mu$ final state. The $\pm1\sigma$ and $\pm2\sigma$ bands around the expected limit are also shown.

$\mu\tau_{\rm h}$, and $e\mu$ final states. The systematic uncertainties for the $e\tau_{\rm h}$, $\mu\tau_{\rm h}$, and $e\mu$ analyses are larger than the statistical uncertainties. Figure 6 (right) shows the exclusion region in the MSSM m_{H^+}-$\tan\beta$ parameter space obtained from the combined analysis for the MSSM $m_{\rm h}^{max}$ scenario [47].

The $t \to H^+b$ branching fraction is calculated with the FeynHiggs program [48]. The exclusion contours corresponding to the $\pm1\sigma$ theoretical error on $\mathscr{B}(t \to H^+b)$ due to missing one-loop EW corrections (5%), missing two-loop QCD corrections (2%) and Δ_b induced uncertainties (the Δ_b term accumulates the SUSY-QCD corrections) [37] are also shown in Fig. 6 (right).

The upper limit on the the branching fraction $\mathscr{B}(t \to H^+b)$ and the exclusion region in the MSSM m_{H^+}-$\tan\beta$ parameter space obtained from the combined analysis are comparable with the

Table 3: The expected range and observed 95% CL upper limit for $\mathscr{B}(t \to H^+b)$ as a function of m_{H^+} for the combination of the fully hadronic, $e\tau_h$, $\mu\tau_h$, and $e\mu$ final states.

95% CL upper limit on $\mathscr{B}(t \to H^+b)$						
m_{H^+}	Expected limit					Observed
(GeV)	-2σ	-1σ	median	$+1\sigma$	$+2\sigma$	limit
80	0.018	0.022	0.029	0.040	0.054	0.041
100	0.014	0.018	0.024	0.032	0.043	0.035
120	0.013	0.015	0.028	0.027	0.040	0.028
140	0.009	0.011	0.014	0.021	0.030	0.022
150	0.008	0.010	0.013	0.019	0.027	0.023
160	0.008	0.009	0.011	0.016	0.023	0.019

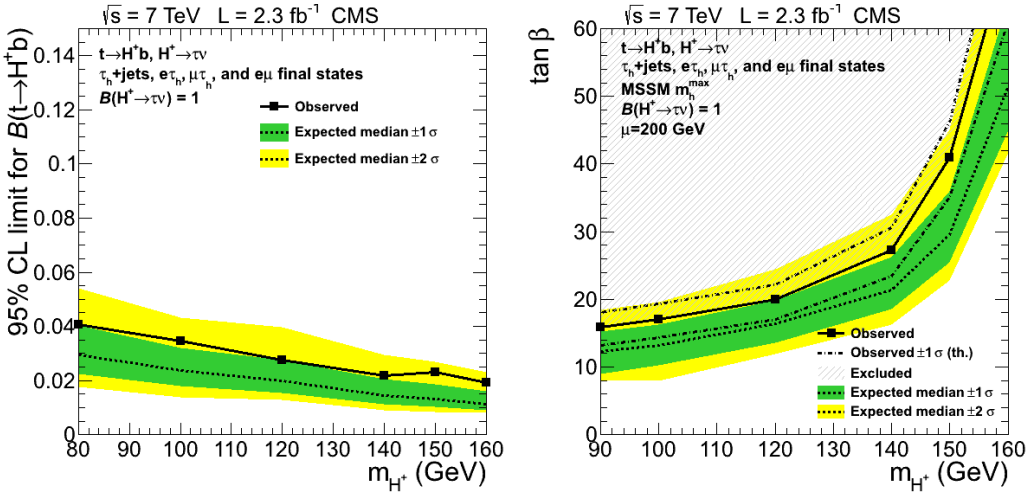

Figure 6: Left: the upper limit on $\mathscr{B}(t \to H^+b)$ as a function of m_{H^+} obtained from the combination of the all final states. Right: the exclusion region in the MSSM M_{H^+}-tanβ parameter space obtained from the combined analysis for the MSSM m_h^{max} scenario [47]. The $\pm1\sigma$ and $\pm2\sigma$ bands around the expected limit are also shown.

results from the ATLAS experiment [17].

7. Summary

A search has been performed for a light charged Higgs boson produced in top quark decays $t \to H^+b$ and which in turn decays into $\tau^+\nu_\tau$. The data sample used in the analysis corresponds to an integrated luminosity of about $2\,\text{fb}^{-1}$. The fully hadronic, $e\tau_h$, $\mu\tau_h$, and $e\mu$ final states have been used in the analysis. The results from these analyses have been combined to extract limits on $t \to H^+b$ branching fraction. Upper limits on the branching fraction $\mathscr{B}(t \to H^+b)$ in the range of 2–3% are established for charged Higgs boson masses between 80 and 160 GeV, under the assumption that $\mathscr{B}(H^+ \to \tau^+\nu_\tau) = 1$.

References

[1] P. Fayet, *Supergauge invariant extension of the Higgs mechanism and a model for the electron and its neutrino*, *Nucl. Phys. B* **90** (1975) 104, DOI10.1016/0550-3213(75)90636-7.

[2] P. Fayet, *Supersymmetry and weak, electromagnetic and strong interactions*, *Phys. Lett. B* **64** (1976) 159, DOI10.1016/0370-2693(76)90319-1.

[3] P. Fayet, *Spontaneously broken supersymmetric theories of weak, electromagnetic and strong interactions*, *Phys. Lett. B* **69** (1977) 489, DOI10.1016/0370-2693(77)90852-8.

[4] S. Dimopoulos and H. Georgi, *Softly broken supersymmetry and SU(5)*, *Nucl. Phys. B* **193** (1981) 150, DOI10.1016/0550-3213(81)90522-8.

[5] N. Sakai, *Naturalness in supersymmetric GUTS*, *Z. Phys. C* **11** (1981) 153, DOI10.1007/BF01573998.

[6] K. Inoue, A. Kakuto, H. Komatsu et al., *Low-Energy Parameters and Particle Masses in a Supersymmetric Grand Unified Model*, *Prog. Theor. Phys.* **67** (1982) 1889, DOI10.1143/PTP.67.1889. Revised version.

[7] K. Inoue, A. Kakuto, H. Komatsu et al., *Aspects of Grand Unified Models with Softly Broken Supersymmetry*, *Prog. Theor. Phys.* **68** (1982) 927, DOI10.1143/PTP.68.927.

[8] K. Inoue, A. Kakuto, H. Komatsu et al., *Renormalization of Supersymmetry Breaking Parameters Revisited*, *Prog. Theor. Phys.* **71** (1984) 413, DOI10.1143/PTP.71.413.

[9] J. F. Gunion, H. E. Haber, G. L. Kane et al., *The Higgs Hunters's Guide*. Westview Press, 2000.

[10] A. Djouadi, *The anatomy of electro-weak symmetry breaking. II. The Higgs bosons in the minimal supersymmetric model*, *Phys. Rept.* **459** (2008) 1, DOI10.1016/j.physrep.2007.10.005, arXiv:hep-ph/0503173.

[11] L3 Collaboration, *Search for charged Higgs bosons at LEP*, *Phys. Lett. B* **575** (2003) 208–220, DOI10.1016/j.physletb.2003.09.057, arXiv:hep-ex/0309056.

[12] ALEPH Collaboration, *Search for charged Higgs bosons in e^+e^- collisions at energies up to $\sqrt{s}$ = 209 GeV*, *Phys. Lett. B* **543** (2002) 1–13, DOI10.1016/S0370-2693(02)02380-8, arXiv:hep-ex/0207054.

[13] DELPHI Collaboration, *Search for charged Higgs bosons at LEP in general two Higgs doublet models*, *Eur. Phys. J. C* **34** (2004) 399–418, DOI10.1140/epjc/s2004-01732-6, arXiv:hep-ex/0404012. 42 pages, 19 figures, Accepted by Eur. Phys. J. C Report-no: CERN-EP/2003-064 Journal-ref: Eur. Phys. J. C34 (2004) 399-418.

[14] OPAL Collaboration, *Search for Charged Higgs Bosons in e+e- Collisions at $\sqrt{s}$ = 189 GeV–209 GeV*, (2008). arXiv:0812.0267. Submitted to *Eur. Phys. J. C*.

[15] CDF Collaboration, *Search for charged Higgs bosons from top quark decays in $p\bar{p}$ collisions at $\sqrt{s} =$ 1.96-TeV*, *Phys. Rev. Lett.* **96** (2006) 042003, DOI10.1103/PhysRevLett.96.042003, arXiv:hep-ex/0510065.

[16] D0 Collaboration, *Search for charged Higgs bosons in top quark decays*, *Phys. Lett. B* **682** (2009) 278, DOI10.1016/j.physletb.2009.11.016, arXiv:0908.1811.

[17] ATLAS Collaboration, *Search for charged Higgs bosons decaying via $H+ \to \tau\nu$ in top quark pair events using pp collision data at $\sqrt{s} = 7$ TeV with the ATLAS detector*, (2012). arXiv:1204.2760. Submitted to *JHEP*.

[18] CMS Collaboration, *Search for a light charged Higgs boson in top quark decays in pp collisions at $\sqrt{s}$ = 7 TeV* , *J. High Energy Phys.* **07** (2012) 143, DOI10.1007/JHEP07(2012)143, arXiv:1205.5736.

[19] CMS Collaboration, *The CMS experiment at the CERN LHC*, *JINST* **03** (2008) S08004, DOI10.1088/1748-0221/3/08/S08004.

[20] CMS Collaboration, *Performance of muon identification in pp collisions at $\sqrt{s}$ = 7 TeV*, CMS Physics Analysis Summary CMS-PAS-MUO-10-002, (2010).

[21] CMS Collaboration, *Electron reconstruction and identification at $\sqrt{s}$~=~7 TeV*, CMS Physics Analysis Summary CMS-PAS-EGM-10-004, (2010).

[22] CMS Collaboration, *Commissioning of the particle flow reconstruction in minimum-bias and jet events from pp collisions at 7 TeV*, CMS Physics Analysis Summary CMS-PAS-PFT-10-002, (2010).

[23] M. Cacciari, G. P. Salam, and G. Soyez, *The anti-k_T jet clustering algorithm*, *JHEP* **04** (2008) 063, DOI10.1088/1126-6708/2008/04/063, arXiv:0802.1189.

[24] CMS Collaboration, *Performance of the b-jet identification in CMS*, CMS Physics Analysis Summary CMS-PAS-BTV-11-001, (2011).

[25] CMS Collaboration, *Performance of τ-lepton reconstruction and identification in CMS*, *JINST* **07** (2012) P01001, DOI10.1088/1748-0221/7/01/P01001.

[26] F. Maltoni and T. Stelzer, *MadEvent: Automatic event generation with MadGraph*, *JHEP* **02** (2003) 027, DOI10.1088/1126-6708/2003/02/027, arXiv:hep-ph/0208156.

[27] J. Alwall, M. Herquet, F. Maltoni et al., *MadGraph 5: going beyond*, *JHEP* **1106** (2011) 128, DOI10.1007/JHEP06(2011)128, arXiv:1106.0522.

[28] T. Sjöstrand, S. Mrenna, and P. Z. Skands, *PYTHIA 6.4 physics and manual*, *JHEP* **05** (2006) 026, DOI10.1088/1126-6708/2006/05/026, arXiv:hep-ph/0603175.

[29] S. Frixione, P. Nason, and C. Oleari, *Matching NLO QCD computations with parton shower simulations: the POWHEG method*, *JHEP* **0711** (2007) 070, DOI10.1088/1126-6708/2007/11/070, arXiv:0709.2092.

[30] Z. Was, *TAUOLA the library for tau lepton decay, and KKMC / KORALB / KORALZ status report*, *Nucl. Phys. Proc. Suppl.* **98** (2001) 96, DOI10.1016/S0920-5632(01)01200-2, arXiv:hep-ph/0011305.

[31] GEANT4 Collaboration, *GEANT4—a simulation toolkit*, *Nucl. Instrum. Meth. A* **506** (2003) 250, DOI10.1016/S0168-9002(03)01368-8.

[32] J. Allison et al., *Geant4 developments and applications*, *IEEE Trans. Nucl. Sci.* **53** (2006) 270, DOI10.1109/TNS.2006.869826.

[33] R. Field, *Early LHC Underlying Event Data – Findings and Surprises*, (2010). arXiv:1010.3558.

[34] U. Langenfeld, S. Moch, and P. Uwer, *New results for $t\bar{t}$ production at hadron colliders*, (2009). arXiv:0907.2527.

[35] N. Kidonakis, *Next-to-next-to-leading soft-gluon corrections for the top quark cross section and transverse momentum distribution*, *Phys. Rev. D* **82** (2010) 114030, DOI10.1103/PhysRevD.82.114030, arXiv:1009.4935.

[36] M. Cacciari, S. Frixione, M. L. Mangano et al., *Updated predictions for the total production cross sections of top and of heavier quark pairs at the Tevatron and at the LHC*, *JHEP* **0809** (2008) 127, DOI10.1088/1126-6708/2008/09/127, arXiv:0804.2800.

[37] LHC Higgs Cross Section Working Group Collaboration, *Handbook of LHC Higgs Cross Sections: 2. Differential Distributions*, CERN Report CERN-2012-002, (2012).

[38] CMS Collaboration, *Measurement of the $t\bar{t}$ production cross section in pp collisions at 7 TeV in* lepton + jets *events using b-quark jet identification*, *Phys. Rev. D* **84** (2011) 092004, DOI10.1103/PhysRevD.84.092004.

[39] ATLAS Collaboration, *Measurement of the cross section for top-quark pair production in pp collisions at $\sqrt{s} = 7$ TeV with the ATLAS detector using final states with two high-pt leptons*, (2012). arXiv:1202.4892. Submitted to *JHEP*.

[40] D. P. Roy, *The Hadronic tau decay signature of a heavy charged Higgs boson at LHC*, *Phys. Lett. B* **459** (1999) 607, DOI10.1016/S0370-2693(99)00724-8, arXiv:hep-ph/9905542.

[41] CMS Collaboration, *Measurement of the top quark pair production cross section in pp collisions at $\sqrt{s}$ = 7 TeV in dilepton final states containing a τ*, (2012). arXiv:1203.6810. Submitted to *PRD*.

[42] CMS Collaboration, *Measurement of the $t\bar{t}$ production cross section and the top quark mass in the dilepton channel in pp collisions at $\sqrt{s} = 7$ TeV*, *JHEP* **1107** (2011) 049, DOI10.1007/JHEP07(2011)049, arXiv:1105.5661.

[43] CMS Collaboration, *Determination of the jet energy scale in CMS with pp collisions at $\sqrt{s}$~=~7~TeV*, CMS Physics Analysis Summary CMS-PAS-JME-10-010, (2010).

[44] L. Read, *Presentation of search results: the CL_s technique*, *J. Phys. G: Nucl. Part. Phys.* **28** (2002) 2693, DOIdoi:10.1088/0954-3899/28/10/313.

[45] T. Junk, *Confidence level computation for combining searches with small statistics*, *Nucl. Instrum. Meth. A* **434** (1999) 435, DOI10.1016/S0168-9002(99)00498-2, arXiv:hep-ex/9902006.

[46] ATLAS and CMS Collaborations, LHC Higgs Combination Group, *Procedure for the LHC Higgs boson search combination in Summer 2011*, ATL-PHYS-PUB/CMS NOTE 2011-11, 2011/005, (2011).

[47] M. S. Carena, S. Heinemeyer, C. E. M. Wagner et al., *Suggestions for improved benchmark scenarios for Higgs- boson searches at LEP2*, (1999). arXiv:hep-ph/9912223.

[48] T. Hahn, S. Heinemeyer, W. Hollik et al., *FeynHiggs: A program for the calculation of MSSM Higgs-boson observables - Version 2.6.5*, *Comput. Phys. Commun.* **180** (2009) 1426, DOI10.1016/j.cpc.2009.02.014.